RESEARCH ARTICLE | JANUARY 18 2024

Water droplet absorption into cellulose-based fabric: A molecular viewpoint FREE

Iwan H. Sahputra ✉; Indar Sugiarto; Hariyo P. S. Pratomo; Andreas Liudi Mulyo

AIP Conf. Proc. 2951, 050005 (2024)
https://doi.org/10.1063/5.0181379

Water Droplet Absorption into Cellulose-based Fabric: A Molecular Viewpoint

Iwan H. Sahputra[1, a)], Indar Sugiarto[1, b)], Hariyo P.S. Pratomo[1, c)], and Andreas Liudi Mulyo[2, d)]

[1]*Faculty of Industrial Technology, Petra Christian University*
Jl. Siwalankerto 121-131, Surabaya 60236, Indonesia
[2]*Department of Electronic Systems, Norwegian University of Science and Technology, NO-7491 Trondheim, Norway*

[a)] Corresponding author: iwanh@petra.ac.id
[b)] indi@petra.ac.id, [c)] hariyo_p@petra.ac.id, [d)] andreas.liudi-mulyo@ntnu.no

Abstract. In this paper, we present the mechanisms of water droplet absorption into the cellulose-based fabric from a molecular viewpoint. A 5×5×5-unit-cells of cellulose Iβ model and a water molecule model have been developed to represent fabric and water droplet. The climbing-image nudged elastic band method was used to find the minimum energy path and the energy barrier of a water molecule when absorbed into three different cellulose surfaces, i.e. [100], [010], and [001] surfaces. The [010] has the lowest calculated energy barrier compared to the other surfaces, thus it is the easiest surface to be penetrated by water molecules. The other surfaces have larger energy barrier values due to the temporary binding of an oxygen atom of the water molecule on cellulose molecules when the water molecule penetrates the surface. For all surfaces, there is not any chemical reaction taking place when the water molecule is adsorbed on the surface or when it is absorbed in the subsurface. Thus, the absorption processes observed in this study is physical absorption.

INTRODUCTION

One of the efforts to suppress the spread of the Covid-19 virus is the use of face masks. If worn properly, wearing a face mask helps prevent droplets that may contain the Covid-19 virus from entering the body through the nose or mouth. Wearing a face mask also helps reduce the exposure of the wearer's droplets (from saliva or breath) to other people in the vicinity. Non-medical face masks widely used by the public are made of several types of fabrics, such as cotton, silk, chiffon, flannel, and their combination. However, the knowledge about the ability of these fabrics to inhibit droplet dispersal is sparse. Likewise, there is a lack of reference about the detailed mechanism of how droplets are absorbed and penetrate the aforementioned fabrics. An understanding of this mechanism is therefore important for the production of new fabric types or mask designs based on existing fabric types. In the end, this could increase the efficiency of the face mask to suppress droplet penetration.

Molecular modelling and simulations have been used to study the adsorption and penetration of oil droplets on cellular membranes [1], water droplets falling on a superhydrophobic surface [2], surface wetting of the crystal structure of cotton cellulose [3], and dynamics of water in microcrystalline cellulose [4].The same approach is employed in this research to investigate the process of absorption of water droplets on cotton-based fabric. Cotton fabric is made from the natural fibers of the cotton plant. This cotton fiber is cellulose which has the chemical formula $(C6H10O5)_n$. There are four types of cellulose, namely cellulose I, II, III, and IV, of which the most common is cellulose I [5]. There are two types of cellulose type I, namely cellulose Iα which is found in metastable conditions, and cellulose Iβ which is more stable [6]. Therefore, the cellulose Iβ model will be employed to represent the cotton fabric in this study. The droplets will be represented by a water molecule (H2O) model.

Proceedings of the 2nd International Conference on Automotive, Manufacturing, and Mechanical Engineering (IC-AMME 2021)
AIP Conf. Proc. 2951, 050005-1–050005-5; https://doi.org/10.1063/5.0181379
Published by AIP Publishing. 978-0-7354-4202-3/$30.00

METHODS

Modeling

A 5×5×5-unit-cells of cellulose-based fabric model was created using the Crystalline Cellulose - Atomistic Toolkit [7]. The model contains 12810 atoms. The unit cell atomic coordinates of the model are from cellulose Iβ which were determined by synchrotron X-ray and neutron diffraction studies [8]. Figure 1 shows, e.g., the [100] surface of this cellulose model as visualized using Jmol [9].

The ReaxFF force field was based on the parameter set developed for glycine conformers and glycine-water complexes [10]. The force field has been shown to be able to predict the lattice constants, elastic constants, and thermal expansion coefficients of cellulose Iβ with reasonable accuracy [11]. The force field has also been utilized to predict the water diffusion coefficient in micro-crystalline cellulose in close agreement with the experimental values [4].

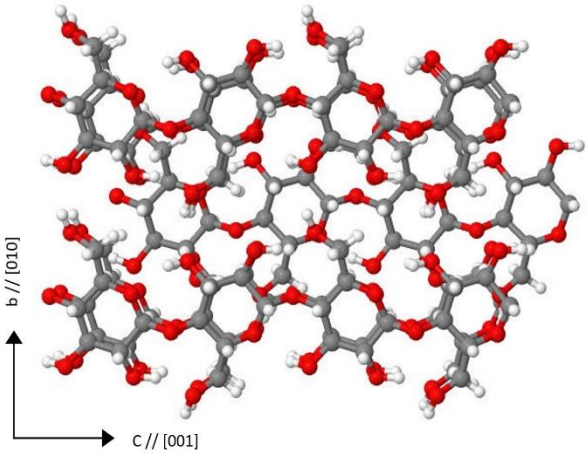

FIGURE 1. The [100] surface of the cellulose model. Red = oxygen atoms, Grey = carbon atoms, White = hydrogen atoms

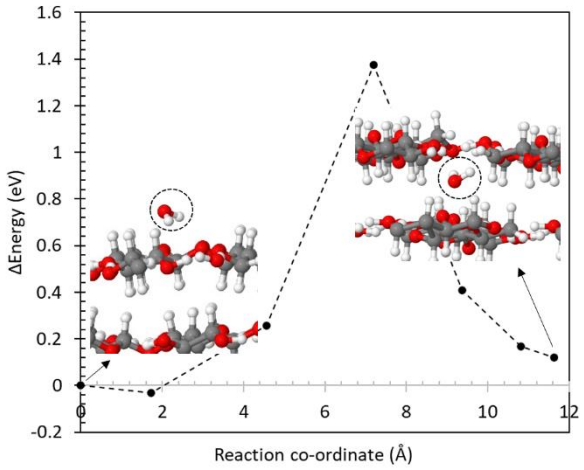

FIGURE 2. Minimum energy path of a water molecule absorption on the [100] surface of the cellulose model. The water molecule is shown inside the dotted circle.

Simulation

The Polak-Ribiere version of the conjugate gradient algorithm [12] was used to minimize the energy of the initial structure with a periodic boundary condition, using a force stopping criteria of 10^{-9}. Three models were created further for [100], [010], and [001] surfaces respectively, by doubling the original simulation box in the respective. The same conjugate gradient algorithm was used to minimize the models with free surfaces. The climbing-image nudged elastic band (CI-NEB) method [13] was used to find the minimum energy path and the energy barrier of a water molecule when absorbed into the cellulose surface. In the CI-NEB, the fast inertial relaxation engine optimization method [14] was used with a force stopping criteria of 1×10^{-3}. The number of images was 7 and a spring constant of 1 was applied in the CI-NEB calculation. The starting configurations were built on the relaxed cellulose with free surfaces as described previously. One water molecule model was inserted randomly on the surface and below the surface respectively. The energy was then minimized by the same conjugate gradient algorithm. Afterwards, system was perturbed further by thermal energy at a temperature of 5 K to find the local minima on the surface and below the surface. The resulting configurations were used as the initial and final points of the transition path in the CI-NEB calculation. All the calculations and simulations described in this section were performed using LAMMPS [15] with periodic boundary conditions.

RESULTS AND DISCUSSION

The minimum energy paths of a water molecule absorption into cellulose surface of [100], [010], and [001] are presented in Fig. 2, 3, and 4. The energy barrier for the absorption process is 1.40 eV, 0.49 eV, and 1.44 eV, respectively.

There is not any comparable energy barrier measurement data for the aforementioned surfaces. However, there is for energy barrier for water diffusion in microcrystalline cellulose with a water moisture content of 20.5%; it was determined to be about 0.32 eV using the nuclear magnetic resonance (NMR) technique [16]. Moreover, for water in cellulose gel (synthesized from sodium cellulose xanthate) with a moisture content of 670% (6.70 g water/g dry gel), the energy barrier was determined to be 0.24 eV using the NMR technique [17]. In addition to that, the energy barrier for water in the cell walls of Sitka spruce (*Picea sitchensis*) decreases from about 0.47 to 0.27 eV as the moisture content increases from 0 to 30%. [18].

The calculated energy barrier for the absorption into [010] surface, i.e., 0.49 eV, is close to the available experimental data for water diffusion in the dry cell walls of Sitka spruce [18] which is 0.47 eV. This is the lowest energy compared to that of other two surfaces. As a consequence, water molecules can penetrate [010] surface much easier than [100] and [001] surfaces.

The locations of the water molecule on the surface of [100], [010], and [001] are presented in Fig. 5, 6, and 7 respectively. These are the preferred sites of water molecules as they are adsorbed on each surface. This is a physisorption or physical adsorption since it does not result in any changes in the chemical bonding structure of water and cellulose. There are van der Waals dan hydrogen bonds between the adsorbed water molecule and the cellulose molecules on the surface. As can be seen from the distances between the water molecule and its nearest hydrogen atoms of the cellulose [19], the hydrogen bonds are strong, moderate, and weak.

When the water molecule is already absorbed in the subsurface, as presented in Fig. 8, 9, and 10 for the surface of [100], [010], and [001] respectively, it does not result in any changes to the chemical bonding structure of water and cellulose. There is not any chemical reaction taking place when the water molecule is in the subsurface, thus it is a physical absorption. Like those on the surfaces, the hydrogen bonds between the water molecule and cellulose in the subsurface are strong, moderate, and weak, as implied from the distances between them [19].

The significant discrepancy in the energy barrier between [010] surface and the other two surfaces is due to the process when the water molecule penetrates the surface, i.e., at the saddle point of the minimum energy path as presented in Fig/ 2, 3, and 4. In the case of [100] and [001] surfaces, one hydrogen of the water molecule is temporarily bonded to one oxygen atom of the cellulose at the saddle point. However, at the next reaction co-ordinate, this bond is broken. In the case of [010] surface, this reaction does not happen.

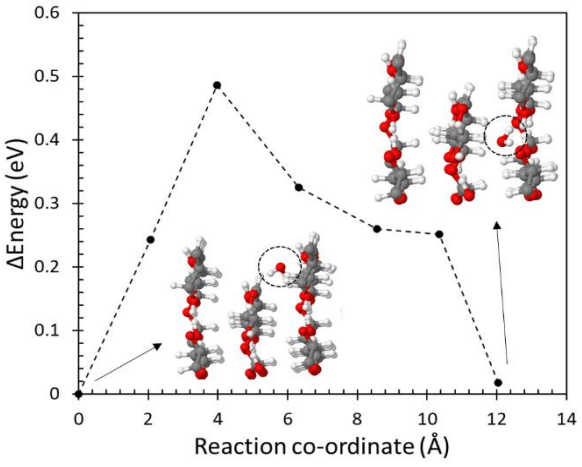

FIGURE 3. Minimum energy path of a water molecule absorption on the [010] surface of the cellulose model. The water molecule is shown inside the dotted circle.

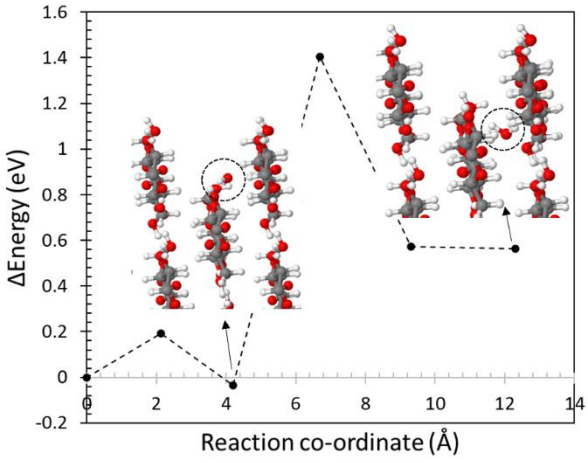

FIGURE 4. Minimum energy path of a water molecule absorption on the [001] surface of the cellulose model. The water molecule is shown inside the dotted circle.

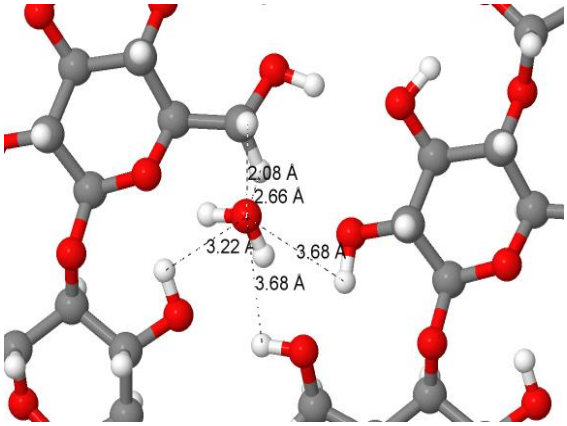

FIGURE 5. Water molecule on the [100] surface of the cellulose (for clarity, only cellulose chains on the surface are shown here) with the distances between its oxygen atom and the nearest hydrogen atoms of cellulose chains.

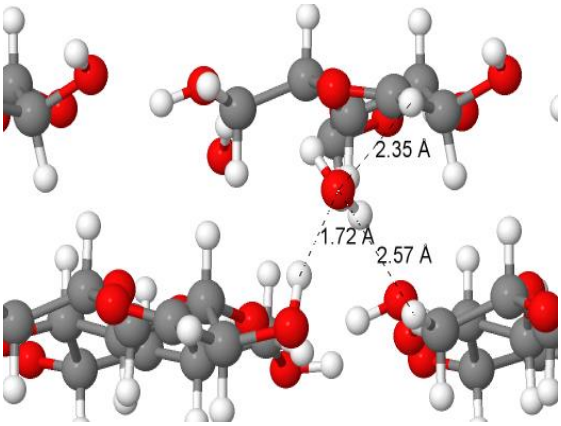

FIGURE 6. Water molecule on the [010] surface of the cellulose with the distances between its oxygen atom and the nearest hydrogen atoms of cellulose chains.

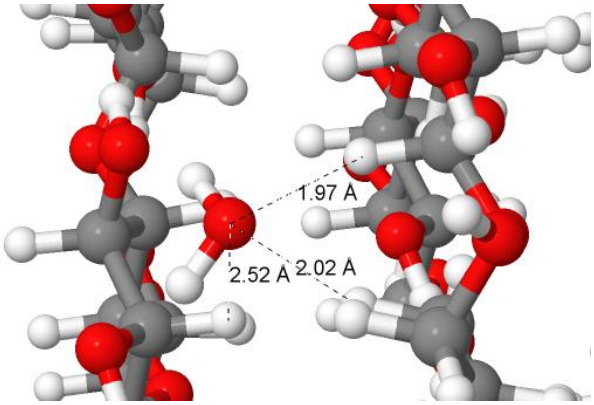

FIGURE7. Water molecule on the [001] surface of the cellulose with the distances between its oxygen atom and the nearest hydrogen atoms of cellulose chains.

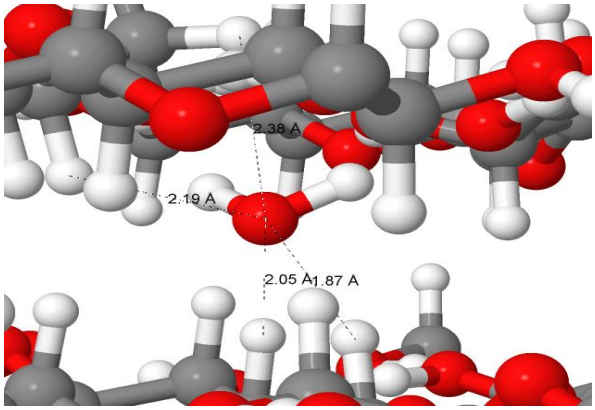

FIGURE8. Water molecule in the [100] subsurface of the cellulose with the distances between its oxygen atom and the nearest hydrogen atoms of cellulose chains.

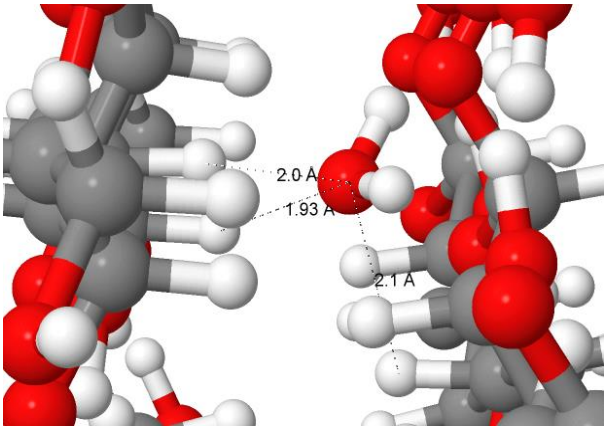

FIGURE9. Water molecule in the [010] subsurface of the cellulose with the distances between its oxygen atom and the nearest hydrogen atoms of cellulose chains.

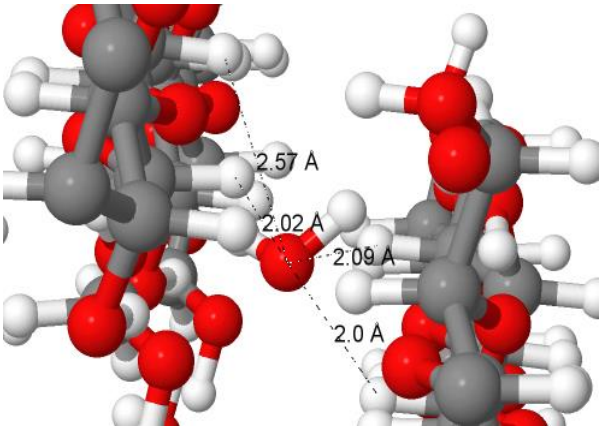

FIGURE10. Water molecule in the [001] subsurface of the cellulose with the distances between its oxygen atom and the nearest hydrogen atoms of cellulose chains.

CONCLUSION

Water molecules penetrate [100] and [001] surfaces of cellulose much harder than [010] surface. This is due to the higher energy barrier of the water absorption into [100] and [001] surfaces compared to [010] surface. There is not any chemical reaction taking place when the water molecule is adsorbed on surfaces and absorbed in sub-surfaces. The significant discrepancy in the energy barrier between surfaces is due to the temporary binding of an oxygen atom of the water molecule on cellulose molecule when water molecule penetrates surface in case of [100] and [001] surfaces. Such phenomenon is not observed in the case of [010] surface. New fabric can be developed using cellulose fibers with substantial [010] and [001] surfaces oriented toward the exterior of the fabric. Face masks made using this fabric will have a higher efficiency to prevent droplets' penetration.

ACKNOWLEDGMENT

This research was supported partially by Lembaga Penelitian dan Pengabdian kepada Masyarakat Universitas Kristen Petra (grant no: 04/HBK-PENELITIAN/LPPM-UKP/XI/2020).

REFERENCES

1. L. Tian and G. Wu, Journal of Hazard. Materials, 122683, (2020).
2. H. Li and K. Zhang, Applied Surface Science **498**, 143793, (2019).
3. P. Venkataraman, H. Ashbaugh, G. P. Johnson, and A. D. French. "Simulation studies of the wetting of icrystalline faces of cotton cellulose," in *Beltwide Cotton Conferences*, 2010, pp. 1577-1580.
4. I. H. Sahputra, A. Alexiadis, and M. J. Adams, Journal of Polymer Science Part B **57**(8), 454-464, (2019).
5. M. Wada, L. Heux, and J. Sugiyama, Biomacromolecules **5**(4), 1385-1391 (2004).
6. J. Sugiyama, J. Persson, and H. Chanzy, Macromolecules **24**(9), 2461-2466 (1991).
7. M. G. Zuluaga, R. J. Moon, F. L. Dri, and P. D. Zavattieri. Crystalline Cellulose - Atomistic Toolkit, (2014).
8. Y. Nishiyama, P. Langan, and H. Chanzy, Journal of the American Chemical Society **124**(31), 9074 (2002).
9. Jmol: an open-source Java viewer for chemical structures in 3D, available at http://www.jmol.org/
10. O. Rahaman, A. C. T. van Duin, W. A. Goddard, and D. J. Doren, The Journal of Physical Chemistry B **115**(2), 249-261 (2011).
11. F. L. Dri, X. Wu, R. J. Moon, A. Martini, and P. D. Zavattieri, Computational Materials Science **109**, 330-340 (2015).
12. E. Polak and G. Ribiere, ESAIM: Mathematical Modelling and Numerical Analysis **3**(16), 35-43 (1969).
13. G. Henkelman, B. P. Uberuaga, and H. Jónsson, The Journal of Chemical Physics **113**(22), 9901, (2000).
14. E. Bitzek, P. Koskinen, F. Gähler, M. Moseler, and P. Gumbsch, Physical Review Letters **97**(17), 170201 (2006).
15. S. Plimpton, Journal of Computational Physics **117**(1), 1-19 (1995).
16. H. Peemoeller and A. R. Sharp, Polymer **26**(6), 859-864, (1985).
17. B. Nyström, M. E. Moseley, W. Brown, and J. Roots, Journal of Applied Polymer Science **26**(10), 3385-3393 (1981).
18. R. M. Nelson, Wood Science and Technology **20**(4), 309-328 (1986).
19. G. A. Jeffrey, *An Introduction to Hydrogen Bonding* (Oxford University Press, 1997).